Effects of neutron irradiation on polycrystalline $Mg^{11}B_2$

C. Tarantini,[1,*] H. U. Aebersold,[2] V. Braccini,[1] G. Celentano,[3] C. Ferdeghini,[1] V. Ferrando,[1] U. Gambardella,[4] F. Gatti,[5] E. Lehmann,[2] P. Manfrinetti,[6] D. Marré,[1] A. Palenzona,[6] I. Pallecchi,[1] I. Sheikin,[7] A. S. Siri,[1] and M. Putti[1]

[1]*INFM-LAMIA/CNR, Dipartimento di Fisica, Via Dodecaneso 33, 16146 Genova, Italy*

[2]*Paul Scherrer Institut, Deptm.Spallation Neutron Source SINQ, CH-5232 Villigen, Switzerland*

[3]*Superconductivity Section, ENEA Research Center, Via E. Fermi 65, Frascati, 00044, Italy*

[4]*INFN Frascati National Laboratory, Via E. Fermi 40, Frascati, 00044, Italy*

[5]*Dipartimento di Fisica, Via Dodecaneso 33, 16146 Genova, Italy*

[6]*INFM-LAMIA/CNR, Dipartimento di Chimica e Chimica Industriale, Via Dodecaneso 31, 16146 Genova, Italy*

[7]*GHMFL, CNRS, 25 Avenue des Martyrs, BP 166, 38042 Grenoble, France*

(Received 28 November 2005; revised manuscript received 1 February 2006; published 27 April 2006)

We studied the influence of the disorder introduced in polycrystalline MgB_2 samples by neutron irradiation. To circumvent self-shielding effects due to the strong interaction between thermal neutrons and ^{10}B we employed isotopically enriched ^{11}B which contains 40 times less ^{10}B than natural B. The comparison of electrical and structural properties of different series of samples irradiated in different neutron sources, also using Cd shields, allowed us to conclude that, despite the low ^{10}B content, the main damage mechanisms are caused by thermal neutrons, whereas fast neutrons play a minor role. Irradiation leads to an improvement in both upper critical field and critical current density for an exposure level in the range $1-2\times10^{18}$ cm^{-2}. With increasing fluence the superconducting properties are depressed. An in-depth analysis of the critical field and current density behavior has been carried out to identify what scattering and pinning mechanisms come into play. Finally, the correlation between some characteristic lengths and the transition widths is analyzed.

DOI: 10.1103/PhysRevB.73.134518 PACS number(s): 74.70.Ad, 61.80.Hg

I. INTRODUCTION

Since its discovery in 2001,[1] magnesium diboride has been one of the most widely studied superconductors. Although as early as in 1959 theoretical works predicted the multigap and multiband features[2] and in 1980 two-band superconductivity was clearly observed in doped $SrTiO_3$ by tunneling measurements,[3] only magnesium diboride presents a spectacular two gap behavior in a favorable range of temperatures.

It was theoretically and experimentally demonstrated that the introduction of disorder can heavily modify the basic MgB_2 properties. It was predicted that interband scattering, induced by nonmagnetic impurities, produces pair breaking and suppresses the critical temperature down to 20 K;[4] intraband scattering, instead, affects resistivity and leads to a change in the shape of upper critical field[5,6] which can exhibit a very different behavior as compared to BCS predictions. Different approaches have been tried in order to increase upper critical field and critical current density without significantly changing the critical temperature with the main purpose of improving the properties of this material for technical applications. The usual way to do this is the chemical substitution on either magnesium or boron sites in order to selectively affect the two intraband electron diffusivities. Although MgB_2 has a very simple crystalline structure, it is not easy to dope; only a few experiments have been successful. Some of them, carried out in single crystals,[7] wires[8] or thin films,[9] have shown that carbon doping in the boron site significantly enhances H_{c2} and at the same time it decreases the anisotropy. Aluminium substitution on the magnesium site either in bulk or single crystal samples gives a clear evidence of a gradual suppression of the upper critical field.[10,11] With both the substitutions critical temperature is suppressed, due to different possible causes; in fact it is necessary to take into account the different variations of the density of states (DOS) induced by different charge dopings. Moreover, disorder introduced by doping might enhance interband scattering, also as an effect of structural deformations, and does not allow us to carefully identify the real reasons for the changes in the superconducting properties. These problems can be overcome either by co-doping, as attempted with a substitution of lithium and aluminium on Mg sites by Monni *et al.*[12] that, nevertheless, did not obtain a complete charge balance, or by particles irradiation.

With regard to particles irradiation, different kinds of experiments using α particles, heavy ions, protons or neutrons have been presented in the literature. The first two methods have been used on MgB_2 thin films. Damage by α particles has been carried out by Gandikota *et al.*,[13,14] who found a gradual T_c suppression and resistivity increase. 200 MeV Ag ions instead have been used by Shinde *et al.*,[15] who observed that the critical temperature remains nearly unchanged, while there is a slight critical current improvement in a narrow range of magnetic fields. Concerning protons irradiation, both bulk and single crystals have been damaged.[16,17] In order to obtain a uniform defects distribution, it is necessary to vary the protons energy that determines the penetration depth. This method leads to an improvement of the J_c field dependence as well as to a significant increase of the irreversibility field which is not accompanied by a significant T_c suppression.

Neutron irradiation has been extensively studied and has shown to be very effective in introducing defects in MgB_2 which are able to improve the superconducting properties and also in suppressing the critical temperature strongly.[18–22]

 ©2006 The American Physical Society

In Refs. 18 and 19 the annealing of defects produced by neutron irradiation has been investigated. Wilke[19] has irradiated MgB_2 wires with fluences ranging between 4.75×10^{18} and 1.9×10^{19} cm^{-2}, obtaining a critical temperature lower than 5 K even in the least irradiated samples. Then, the superconductive properties have been systematically studied as a function of annealing temperature and time; using this procedure only slight H_{c2} and J_c improvement with respect to those of the pristine samples has been observed.

In general neutron irradiation suffers of the inhomogeneity problem due to the huge cross section of neutron capture by ^{10}B whose consequence is the short penetration depth of thermal neutrons in MgB_2. In Refs. 20 and 21 this problem has been overcome by using a cadmium shield to absorb the lowest energy neutrons. Another method to avoid inhomogeneous defects distribution in bulk and wires is the choice of sample thickness smaller than the penetration depth.[18,19]

In this work we solve the inhomogeneity problem, inherent in neutrons irradiation, by preparing samples with boron isotopically enriched in ^{11}B, so as to reduce the ^{10}B capture probability and to enlarge the penetration depth, following the idea presented in Ref. 22. We present a wide investigation of superconducting properties for a large series of samples, and we compare our results with those of irradiated samples of literature prepared with natural boron.

II. SAMPLE PREPARATION AND CHARACTERIZATION

The samples for this experiment were prepared by direct synthesis of pure elements with a single step method,[23] using a similar technique as in earlier works.[24,25] Boron and magnesium (99.999% purity) were put in Ta crucibles welded in argon and closed in a quartz tube under vacuum. Then they were heated up to 950 °C to produce dense, clean, and hard cylinder shaped samples. The only peculiarity of these samples, compared to the usually prepared ones, comes from the particular boron used. In fact we employed crystalline isotopically enriched ^{11}B from Eagle-Picher (99.95% purity), with a residual ^{10}B concentration lower than 0.5%. The pristine properties are optimal T_c (39.2 K), sharp superconducting transition (0.2 K), low residual resistivity [$\rho(40) < 2\ \mu\Omega$ cm] and high residual resistivity ratio (RRR $\sim 11-15$). The quality of the MgB_2 phase was initially studied by x-ray powder diffraction with a Guiner-Stoe camera; no extra peaks due to free Mg or spurious phases were detected. The samples were then cut in parallelepiped bars ($\sim 1\times1\times12$ mm^3) and irradiated in different ways.

A. Neutron irradiation

In order to shed light on the different role of fast and thermal neutrons, three series of samples were irradiated at two different facilities. The first series (L series) was irradiated in a TRIGA MARK II type nuclear research reactor (thermal and fast neutron flux density up to 10^{13} cm^{-2} s^{-1} and 1.2×10^{13} cm^{-2} s^{-1}, respectively) at the Laboratory of Applied Nuclear Energy (LENA) of the University of Pavia, reaching a maximum thermal neutron fluence of 10^{18} cm^{-2}. The other two series were irradiated in a spallation neutron source SINQ (thermal and fast neutron flux density up to 1.6×10^{13} cm^{-2} s^{-1} and 10^{10} cm^{-2} s^{-1}, respectively) at the Paul Scherrer Institut (PSI), Villigen. In this latter facility, we exposed MgB_2 samples to neutrons, both with and without Cd shields (P Cd and P series, respectively), for increasing irradiation times, to gradually modify the superconducting properties. To obtain an exposition level of 1.4×10^{20} cm^{-2}, the most irradiated sample was exposed for nearly 4 months. It is worth noticing that these two facilities have approximately the same flux density of thermal neutron, but they differ by three orders of magnitude in the fast neutron flux density.

Fast or thermal neutrons should induce different types of defects as a consequence of their interaction reactions and the corresponding cross sections, which are dependent on the neutron energy. Fast neutrons have large enough energy to undergo direct collisions with nuclei and displace them from their lattice positions, thus producing point defects. However, the cross sections for such events are generally smaller than the ones for thermal neutrons; this means that, in general, thin samples are not strongly influenced by fast neutrons. Thermal neutrons instead have lower energy and the only way they produce disorder is through the neutron capture reaction by ^{10}B; this process causes the isotropic emission of an α particle and a ^{7}Li nucleus, with energy of 1.47 MeV and 0.84 MeV, respectively. Along the range of recoil (4.8 μm and 2.1 μm, respectively) these particles lose energy by interacting with electrons and they create atom displacements mainly at the end of the range. As this capture reaction has a large cross section, if we used natural boron (with 20% of ^{10}B content), the penetration depth would be as small as 200 μm and there would be a shielding effect at the surface. In thicker bars, this should give rise to a much disordered region next to the surface and therefore a gradient in the defects density throughout the sample. We chose to employ isotopically enriched ^{11}B to avoid this problem; in fact with only 0.5% of ^{10}B content, the penetration depth grows up to $\sim$1 cm, becoming larger than our MgB_2 bars thickness.

B. Structural characterization

The general properties of the so-obtained samples are summarized in Table I, where critical temperature, resistive transition width (10%–90% criterion), normal state resistivity, $\Delta\rho=\rho(300\text{ K})-\rho(40)$, residual resistivity ratio RRR $=\rho(300\text{ K})/\rho(40)$, and crystallographic axes at different thermal neutron fluence are reported. In Table I, we report also the data for the cadmium shielded sample; these results will be separately described in a following paragraph.

X-ray diffraction, performed in the standard Bragg-Brentano geometry, allowed us to study the structural properties before and after irradiation. Figure 1 shows the magnification of the (002) and (110) MgB_2 reflections for some irradiated samples of the PSI series. The peaks remain very narrow up to the highest exposition level and the gradual changes in both lattice parameters are evident. The double peak structure is due to Cu $K\alpha1$ and Cu $K\alpha2$ present in the x-ray beam. In order to carefully estimate a and c axes, we performed a Rietveld refinement on the whole x-ray spectra

TABLE I. Main properties for all the irradiated samples: thermal neutron fluence, critical temperature, and transition width [defined as $T_c = T_{50\%}$ and $\Delta T_c = (T_{90\%} - T_{10\%})$], resistivity at 40 K, ρ(40 K), residual resistivity ratio RRR$=\rho$(300 K)/ρ(40 K), lattice parameters a and c.

Samples	Fluence (cm^{-2})	T_c (K)	ΔT_c (K)	ρ(40) ($\mu\Omega$ cm)	$\Delta\rho$ ($\mu\Omega$ cm)	RRR	a (Å)	c (Å)
L-0	0	39.1	0.2	0.7	9.5	15	3.084	3.522
L-1	1.0×10^{15}	39.1	0.2	0.7		15		
L-2	1.0×10^{16}	39.1	0.2	0.7		15		
L-3	1.0×10^{17}	39.1	0.2	2.0	14	8.0	3.086	3.526
L-4	1.0×10^{18}	37.0	0.2	7.7	12	2.5	3.086	3.527
P-0	0	39.1	0.2	1.6	16	11	3.084	3.519
P-1	1.0×10^{17}	38.9	0.3	2.4	14	7.0	3.083	3.524
P-2	6.0×10^{17}	37.7	0.2	6.5	13	3.0	3.085	3.529
P-3	7.6×10^{17}	35.9	0.3	16	15	2.0	3.083	3.525
P-3.5	2.0×10^{18}	33.3	0.3	26	14	1.6	3.088	3.537
P-3.7	5.5×10^{18}	27.3	1.0	41	10	1.3	3.088	3.538
P-4	1.0×10^{19}	23.8	0.9	64	13	1.2	3.088	3.549
P-5	3.9×10^{19}	11.7	0.7	124	15	1.1	3.095	3.558
P-6	1.4×10^{20}	9.1	0.3	130	12	1.1	3.093	3.558
P-Cd1	1.6×10^{18}	39.0	0.2	2.1	15	8.3	3.084	3.521
P-Cd2	5.6×10^{18}	38.9	0.2	1.9	11	6.7	3.086	3.526

for all the samples. In Fig. 2 we report the lattice parameters as a function of the thermal neutron fluence of the sources. The lattice parameters increase following the same trend in both L and P series; the a axis expands by less than 0.4%, whereas the c axis increases by more than 1% (volume change of 1.7%). A similar anisotropic expansion has been observed also by Kar'kin *et al.*,[18] who reported a and c variations of 0.24% and 0.9%, respectively, with a volume increase of 1.4% at 10^{19} cm^{-2} fluence level, comparable to our value of 1.1% at the same irradiation. The behavior presented by Wilke *et al.*[19] is quite different. At just 9.5×10^{18} cm^{-2}, they found an enhancement of volume by 2.6%, greater than the values we obtain in the most irradiated samples. Moreover the authors showed a substantial change in the structural properties of the samples upon irradiation with a strong (002) peak broadening; this trend, observed on the most irradiated samples, is attributed to a change in the correlation length along the c axis. Instead, in the less irradiated wires the peak widths were similar to ours. The (002) peak broadening probably appears at a damage level not yet reached in our samples, as a consequence of our low content of ^{10}B.

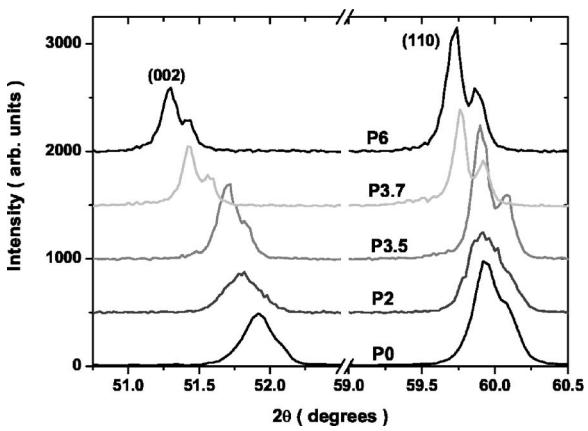

FIG. 1. X-ray diffraction patterns on (002) and (110) reflections for unirradiated (P0) and irradiated (P2, P3.5, P3.7, P6) samples.

C. Electrical characterization

Resistivity and magnetoresistivity were investigated by ac electrical resistance measurements carried out in a 9 T Quantum Design PPMS and then up to 28 T in a resistive magnet at the Grenoble High Magnetic Field Laboratory with a measuring current density of $\sim$1 A/cm^2. The resistivity curves

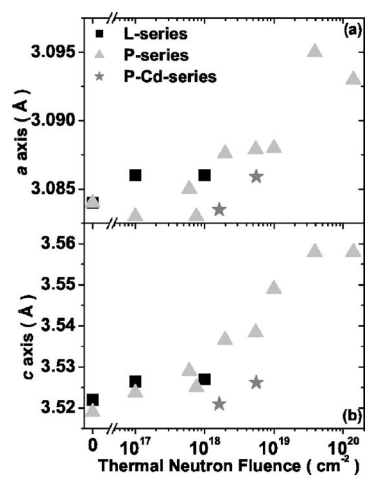

FIG. 2. a and c axes as a function of thermal neutron fluence for L-(black squares), P-(grey triangles), and P-Cd-series (grey stars).

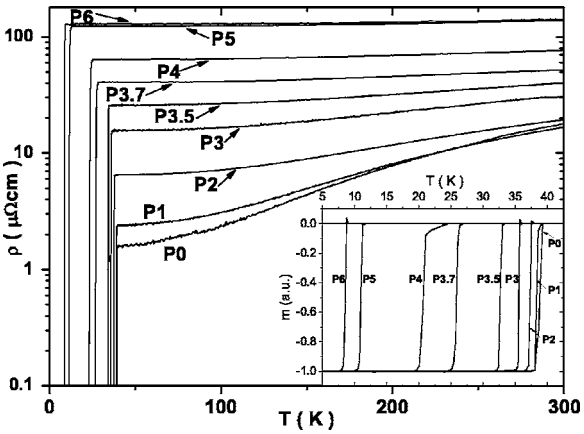

FIG. 3. Resistivity curves as a function of temperature for the P-series; in the inset, the magnetic superconducting transitions are shown as measured in the SQUID.

are plotted in Fig. 3 for the P series; moreover in the inset the susceptibility, measured by Quantum Design SQUID magnetometer in an applied field of 10 Gauss, is shown. The transition widths, measured both by resistivity and susceptibility, remain rather sharp even in the most irradiated samples. Only sample P-4, in the magnetic transition, shows a width larger than 3 K. The overall transition width versus fluence will be discussed in Sec. VI.

In Fig. 4 we plot the critical temperature T_c [Fig. 4(a)] (defined at 50% of the normal state resistivity) and the resistivity ρ at 40 K [Fig. 4(b)] as a function of the thermal neutron fluence. The critical temperature of the P and L series decreases monotonically with the neutron fluence; it is suppressed only by 2 K up to 10^{18} cm^{-2} and then reaches 9.1 K at the highest exposition level. At the same time resistivity grows by more than two orders of magnitude, from $\sim$1 to 130 $\mu\Omega$ cm. The resistivity increase is likely due to an enhancement in intraband scattering, induced by irradiation, which causes a reduction in the electron mean free path. With regard to $\Delta\rho$, it remains approximately constant

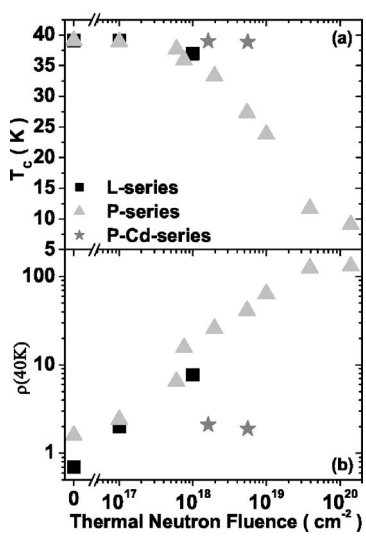

FIG. 4. (a) Critical temperature T_c and (b) resistivity at 40 K, ρ(40 K) as a function of thermal neutron fluence.

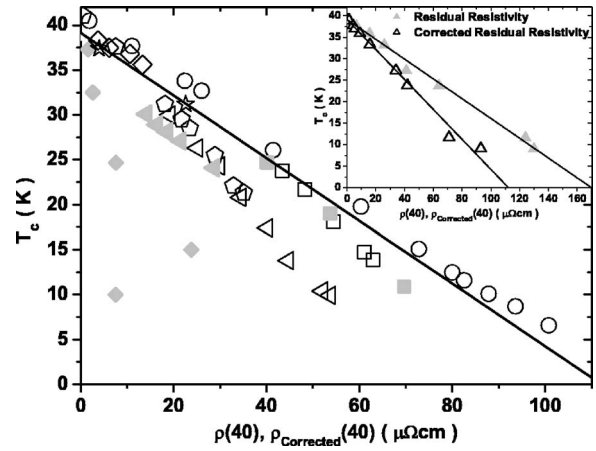

FIG. 5. Critical temperature as a function of residual resistivity from various papers: Ref. 13, (○, open pentagon); Ref. 14, before (□,◁) and after (■,◀) annealing, respectively; Ref. 27, (☆); Ref. 28, (◇); Ref. 19, (◆); the line represents the data of the present work. In the inset, critical temperature versus residual resistivity (full symbols) and versus residual resistivity corrected by Rowell's criterion (open symbols) for all the samples. The line, that represents the best fit of the open symbols, is also reported in the main panel.

($\sim$10–15 $\mu\Omega$ cm) over the whole range of irradiation (see Table I). In Ref. 26 Rowell suggested that in polycrystalline samples $\Delta\rho$ should be nearly equal to 8–9 $\mu\Omega$ cm, while an increasing $\Delta\rho$ in irradiated and substituted samples indicates poor connectivity. In the pristine samples (LENA-0 and PSI-0) we measure generally $\Delta\rho$ values slightly larger (10–12 $\mu\Omega$ cm) than the predicted ones, probably due to the not full density of the samples. Anyway, no systematic increase of $\Delta\rho$ with irradiation is observed, indicating that the produced damages do not significantly affect the connectivity of the samples.[13]

To highlight the direct relationship between ρ and T_c and eliminate the fluence dependence, in the inset of Fig. 5 we plot critical temperature as a function of resistivity (solid symbols). We observe a linear decrease of T_c versus ρ, as already found in MgB_2 thin films irradiated by α particles.[13] Even if we rescale the resistivity data by assuming $\Delta\rho = 8$ $\mu\Omega$ cm as suggested by Rowell,[26] we obtain again a linear behavior (inset of Fig. 5, open symbols). With this correction, we obtain the limit resistivity value, that is 110 $\mu\Omega$ cm, at which $T_c=0$; this resistivity is similar to value obtained in Ref. 13. In the main panel of Fig. 5, we compare our results on T_c versus ρ (black line) with other similar data from literature about samples prepared with natural boron; we considered irradiated and then annealed thin films[13,14] and wires,[19] irradiated bulk,[27] and C-doped wires.[28,29] Almost all these series of samples follow a roughly linear T_c versus ρ behavior with a limit resistivity value ranging between 70 and 120 $\mu\Omega$ cm. In particular, in Gandikota's thin films this behavior is followed both before and after annealing procedure.[14] The only exception is observed in irradiated and successively annealed wires[19] that show very low resistivity values in spite of the large T_c suppression. Interestingly, T_c versus ρ behavior of C-doped

wires[28,29] nearly overlaps data of irradiated samples. As shown in Sec. IV these samples present nearly the same upper critical fields of irradiated ones.

It is worth noting that, differently by the Golubov and Mazin predictions,[4] no saturation is present at 20 K; this means that pair breaking by interband scattering is not the only mechanism that is able to suppress the critical temperature in the irradiated samples. On the other hand, the roughly linear trend of T_c with ρ suggests that a strong correlation exists between the mechanism increasing the resistivity (scattering by atomic scale defects) and those which suppress the critical temperature. This behavior is common to other superconductors. In amorphous transition metals and damaged A15 superconductors, for instance, a smearing of the peak in the electron density of states at the Fermi level was proposed as a mechanism for the T_c reduction;[30] yet, this mechanism cannot simply explain the MgB_2 case, whose density of states is rather flat around the Fermi level; other mechanisms suppressing the electron-phonon coupling should be invoked as well.

III. THERMAL OR FAST NEUTRONS

In the last years several experiments of neutron irradiation have been carried out to understand the effectiveness of thermal and fast neutrons. Nevertheless, up to now, the comprehension of the different effects coming into play is not clear, yet.[19–21]

Now, we point out that both Figs. 2 and 4 are plotted as a function of the thermal neutron fluence. Although the two different neutron sources employed to irradiate the samples differ by three order of magnitude in the fast neutrons flux, both the L and P series follow the same behavior both as for the crystal axes expansion and the change of critical temperature and resistivity. This is evidence that the superconducting properties are effectively changed by thermal neutrons, whereas fast neutrons play a minor role.

To confirm this result we irradiated samples employing a cadmium shield as proposed by Eisterer.[20] As cadmium has a huge cross section for neutrons whose energy is lower than 0.5 eV, this technique can be used to probe the fast neutrons role alone. The properties of such samples have been measured and analyzed as L and P series. The behavior of these samples is quite different from the ones irradiated without shield. Already in the structural characterization (see Fig. 2) we note that lattice parameters of P-Cd1 have no changes compared to the pristine ones. P-Cd2 axes instead only slightly increase. The critical temperature and the resistivity values remain nearly unchanged. We can observe in Table I and Fig. 4 that T_c is suppressed only by 0.2 K in the most irradiated samples, whereas ρ assumes approximately the same values of L-3 and P-1. These data indicate that this series behaves as if it was irradiated with fluences which are nearly 50 times smaller than those used for the L and P series. This effect can be easily explained considering that cadmium shields thermal neutrons and only fast neutrons can reach the samples. We think that this finding confirms that fast neutrons are not very effective in the defect production. Only thermal neutrons and their nuclear reaction with residual ^{10}B should be taken into account to explain the modification of superconducting properties.

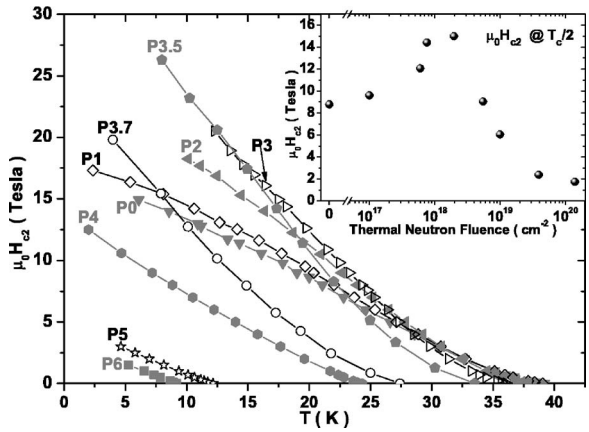

FIG. 6. Upper critical field as a function of temperature estimated at 90% of the resistive transition. The inset shows critical field behavior versus fluence at $T_c/2$ for the P series.

IV. UPPER CRITICAL FIELD

Upper critical field is one of the more interesting properties and, in different experiment, the effect of the irradiation was studied on samples prepared with natural boron both with and without the cadmium shield.[20,21] It was observed that the presence of Cd shield leads to a critical temperature close to the pristine value and an upper critical field only slightly enhanced in the parallel direction. Moreover, Eisterer[21] reported an evident anisotropy reduction in single crystals, induced mainly by an enhancement of H_{c2} in the perpendicular direction. In addition, that work reported also the study on the samples irradiated without the cadmium shield; T_c and consequently also H_{c2} were strongly suppressed, without substantially changing the $H_{c2}(T)$ shape. Wilke *et al.*,[19] indeed, irradiated the samples up to 1.9×10^{19} cm^{-2}, which leads to a suppression of the critical temperature down to 5 K. To restore the superconducting properties, they annealed the samples at different temperatures; in the best case, when the critical temperature was almost completely restored, the upper critical field at 0 K grew from ~16 T in the undamaged sample, to about 19 T. Moreover, the curve shape slightly changed, showing a more marked upward curvature near T_c and assuming a more linear trend at low temperature.

In this work, upper critical field has been evaluated for each temperature as the 90% of the normal state in the resistivity transition. It is worth noting that in polycrystalline samples, with randomly oriented grains, the so estimated values coincide with the largest H_{c2}, that is the critical field parallel to the *ab* plane. In Fig. 6 we report $H_{c2}(T)$ curves; for clarity only *P* series is shown. H_{c2} curves of the Cd shielded one have only a slight improvement compared to the pristine sample, while L-4 behaves similarly to the P-2 curve. Moreover, in our data, the curves are gradually modified by neutron irradiation and they eventually assume a completely different shape. Initially, at low temperature, a

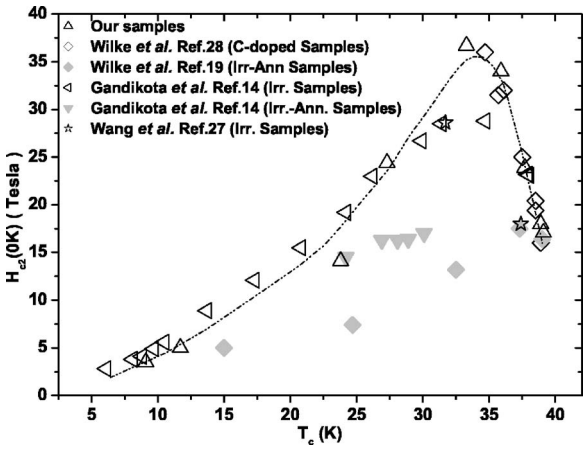

FIG. 7. Upper critical field as a function of critical temperature in irradiated or C-doped samples (open symbols) and in irradiated and then annealed samples (full symbols); the line is only a guide for the eyes.

remarkable downward curvature is observed. Upon irradiation, the slope increases and the behavior becomes almost linear in the P3.5 sample. Here, $H_{c2}(0)$ attains value larger than 30 T, twice as much as that of the pristine sample. With further irradiation, the curves show an upward curvature at low temperature, particularly evident in P3.7 and P4 samples. $H_{c2}(T)$ curves, in samples P5 and P6, are linear in the measured range of temperatures; the extrapolated values at 0 K turn out similar to ones shown in Refs. 14 and 19. In the inset, the critical field at $T_c/2$ versus fluence for the P samples series is plotted. In this graph the effect of irradiation on H_{c2} is emphasized. H_{c2} grows up to a fluence level of 2×10^{18} cm^{-2} (sample P-3.5), where the critical temperature is suppressed by only few degrees; instead, in the most irradiated samples, H_{c2} is suddenly reduced both as a consequence of a strong T_c suppression and of the anisotropy reduction observed in Ref. 21.

As a substantial improvement of upper critical field upon irradiation has been observed, like in carbon doped samples, a comparison between our H_{c2} data and those reported in literature on other disordered samples, could be interesting. In Fig. 7 we report the upper critical field at 0 K, obtained by linear extrapolation, as a function of critical temperature for different literature samples. We considered samples whose critical temperatures and resistivities of the starting materials were similar to ours; thin films irradiated with α particles,[14] carbon substituted wires,[28] neutron irradiated bulks,[27] and wires.[19] All these disordered samples behave similarly; upper critical field presents a maximum, larger then 35 T, when the critical temperature is around 35 K. This behavior was already observed in earlier works[27,22,14,28] and underlined in Refs. 19 and 31. The behavior of samples annealed after irradiation is quite different (full symbols); in fact, both in Gandikota's thin films[14] and in Wilke's wires,[19] the upper critical field remains significantly lower. It appears that annealing is more effective in removing the defects related to the increase of H_{c2}.

In order to understand the H_{c2} behavior, we applied the theoretical model of Refs. 5 and 9, where the Usadel equations for a dirty two-gap anisotropic superconductor are developed. Starting from these equations, the behavior of the upper critical field as a function of temperature is derived. These articles emphasize as interband scattering should be the principal cause for the critical temperature suppression, whereas intraband scattering, and thereby diffusivities ratio ($\eta=D_\pi/D_\sigma$), affects the shape of H_{c2} vs T curves in different temperature ranges. If $\eta>1$, the critical field shows a slight upward curvature near T_c, while at 0 K it exceeds the predicted BCS value; conversely, if $\eta<1$, H_{c2} remains nearly linear in the high temperature region and presents a remarkable upward curvature at low temperature. This model seems to explain the upper critical field behavior,[9,32–34] even if it does not allow us to estimate the resistivity values correctly. If we fix the electron-phonon coupling constants of the pure MgB_2, we can reproduce the shape of the less irradiated samples, as long as T_c is not reduced by more than 6 K and critical field is steadily increased by irradiation. In Table II the fit parameters for $P1$, $P2$, $P3$, and $P3.5$ are summarized; since in bulk samples it is possible to measure the critical field in one direction only, we could solely determine the effective σ-band diffusivity $D_{\sigma\mathrm{Eff}}=(D_\sigma^{ab}D_\sigma^{c})^{0.5}$ and the effective ratio $\eta_{\mathrm{Eff}}=D_\pi/D_{\sigma\mathrm{Eff}}$ (D_π is assumed isotropic). Nevertheless we have an estimation of the anisotropy values from the critical current analysis[35] (as mentioned later on in Sec. V, γ ranges from 4.5 to 4, in the less irradiated samples, to 1, in the most irradiated ones), so we can determine both in-plane and out-of-plane σ-band diffusivities. In all the fits, the critical temperature values are smaller than the experimental ones by 1 or 2 K; this problem does not worsen the fit quality as shown in Fig. 8, where calculated curves are plotted together with data points for P-3 and P-3.5. It turns out that $\eta=D_\pi/D_\sigma^{ab}$ is larger than unity and monotonically decreases from 9.5 to 5.7 with increasing irradiation (see Table II); in

TABLE II. Fit parameters obtained by the H_{c2} model for less irradiated samples of the P-series: $\rho_{0\mathrm{Mis.}}$, resistivity measured at 40 K; η, ratio between diffusivities D_π and D_σ^{ab}; D_σ^{ab}, σ band in-plane diffusivity; D_π, π-band diffusivity; $\rho_{\mathrm{Calc.}}$, resistivity calculated by D_π and D_σ^{ab}; $H_{c2}(0)$, upper critical field at 0 K estimated by the model.

Sample	$\rho_{0\mathrm{Mis.}}$	$\eta=(D_\pi/D_\sigma)$	$D_\pi(\cdot10^{-4})$	$D_\sigma(\cdot10^{-4})$	$\rho_{\mathrm{Calc.}}$	$H_{c2}(0)$
P-1	2.4	9.5	61	6.4	7	16.9
P-2	6.5	8.6	43	4.9	10	21.0
P-3	16	6.0	19	3.2	22	26.5
P-3.5	26	5.7	11	2.0	37	30.2

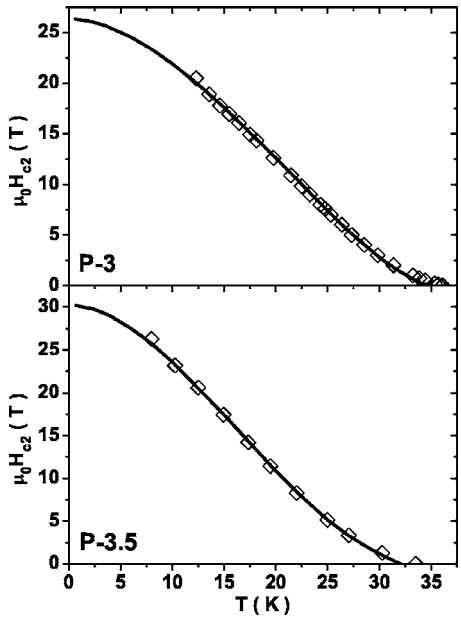

FIG. 8. Upper critical field data (open symbols) and H_{c2} fit curves (solid lines) for P3 and P3.5 samples.

the framework of this model, these η values indicate that the σ band is always dirtier than the π band. Moreover D_{σ}^{ab} and D_{π} are approximately reduced by a factor of 3 and 6, respectively, from $P1$ to $P3.5$; this means that the π band gets dirty faster than the σ band. From D_{π} and D_{σ} we can estimate the residual resistivity; the obtained values, reported in Table II, increase with irradiation as in the measured ones, but they are slightly larger.

However the H_{c2} model does not work in the most irradiated samples, perhaps due to a change in the electron-phonon coupling. Such hypothesis seems to be confirmed by the specific heat studies carried out on these samples;[36] we have noticed that Sommerfeld's constant γ_S remains unchanged ($\sim$3 mJ/mol K^2) in the less irradiated samples, and then decreases to 2.5 mJ/mol K^2 in the most irradiated ones. As γ_S linearly depends on the density of states renormalized by the electron-phonon coupling, the decrease of γ_S can be attributed to a weakening of the coupling. This effect, besides being an explanation for the T_c suppression, can be accountable for the failure of the H_{c2} model. As in the most irradiated samples the coupling constants change, we should take into account this modification to fit the H_{c2} curves. As mentioned above, the P3.7 sample shows a marked upward curvature in H_{c2} in the whole range of temperatures and this trend cannot be explained by this model. In a sample whose critical temperature is so much suppressed indeed, also in the case of $\eta < 1$ the upward curvature should not appear, as a consequence of a large interband scattering. Probably this critical temperature is mainly determined by other mechanisms, rather than by the interband scattering. Instead, in the most irradiated samples, critical temperature is low and no upper curvature is observed near T_c. In Ref. 19 a WHH single gap behavior[37] has been observed in the case of similar critical temperature. In our less irradiated samples, H_{c2} measurements are limited to about $T_c/2$ but the presence of a single gap is supported by specific heat results. In fact they highlight a crossover between two and single gap behavior when critical temperature passes from 21 to 11 K.[36]

The diffusivity parameters that we obtained in the framework of this H_{c2} model produce acceptable fits, at least on the less disordered samples. Nevertheless some caution must be taken into consideration about the diffusivity values. In fact the calculated resistivities, even though they show the same monotonic trend with respect to the measured ones (ρ increases with disorder), do not correspond exactly as for their absolute values. In Ref. 38 the authors suggested that this discrepancy could be induced by an additional extrinsic contribution in the measured resistivity due to grain boundary structure. However, this interpretation cannot be applied in our case because the resistivities estimated by the fit parameters are larger than experimental ones. Moreover, despite it seems reasonable that increasing irradiation the two bands tend to become equally disordered ($\eta \rightarrow 1$), because the disorder should not be preferentially located in the boron or magnesium planes, the fact that, in the less disordered sample, σ band turns out to be dirtier than the π band is a controversial result. In the literature, in general, in clean systems the σ band is believed to be cleaner than a π band,[39] although there are also opposite results.[34] We believe that the above mentioned results need to be confirmed by similar analysis done on critical fields of single crystal or clean epitaxial films where the presence of the two orientations reduces the number of free fit parameters. Recently we demonstrated that high field magnetoresistance[40] is an alternative method in determining the scattering times in the two bands. Work is in progress to perform similar measurements (that need high magnetic fields) on these samples and study the critical fields of irradiated epitaxial thin films.

V. CRITICAL CURRENT DENSITY

In order to examine the effect of neutron irradiation, the critical current density and its behavior in the magnetic field have also been analyzed. The hysteresis loops have been measured in a Quantum Design SQUID magnetometer up to 5 T and in a vibrating sample magnetometer (VSM) up to 12 T. The critical current densities were extracted applying the critical state model. In Fig. 9, we report experimental data of critical current density of all P samples, some of which have been studied in a previous publication.[35] Irradiation, despite suppressing T_c, significantly improves the magnetic field dependence of the critical current density. In the inset of Fig. 9, the trend of J_c versus neutrons fluence at 5 K and 4 T is plotted. Again, like in the H_{c2} behavior described above, this is an indication that the optimized superconducting properties are obtained by irradiating with fluence near 2×10^{18} cm^{-2}, close to the case of the P3.5 sample. This sample has a critical current smaller than P3 up to 4 T; however at this point a crossover occurs and P3.5 shows a strong improvement of its field dependence, reaching a value close to 10^4 A/cm^2 at 10 T.

It is evident that the rise of J_c with irradiation cannot be ascribed to the increase of H_{c2}: at low irradiation levels (10^{17} cm^{-2}), despite the fact that the upper critical field does not change significantly, the field dependence of J_c is

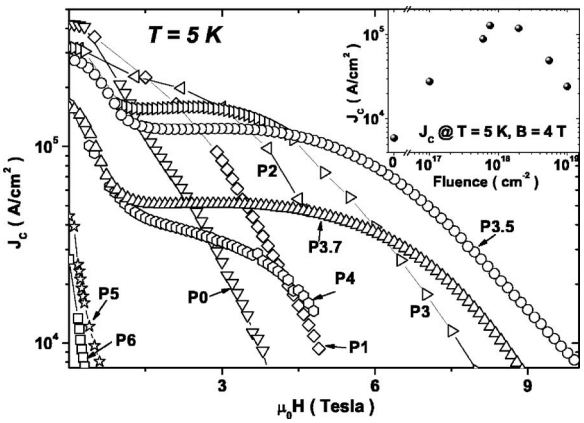

FIG. 9. In the main panel, critical current density at 5 K as a function of magnetic field and as a function of fluence at 4 T, in the inset.

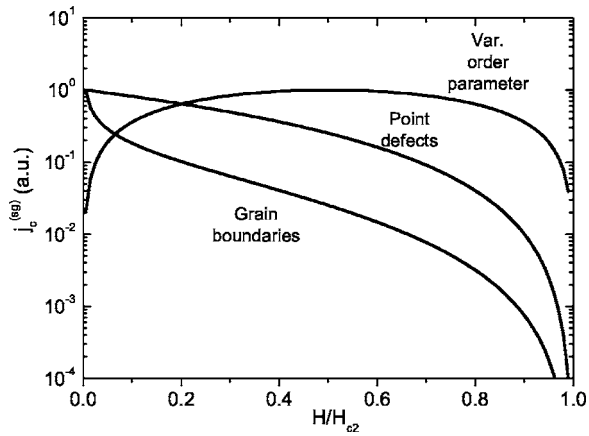

FIG. 10. Single grain critical current density from three different pinning mechanisms (grain boundaries, point defects, and variations of the superconducting order parameter) as a function of the reduced field H/H_{c2}. The curves are normalized to the respective maximum values.

strongly affected by irradiation. Indeed, by applying Eisterer's percolative model,[41] we have demonstrated quantitatively that neutron irradiation induces a new pinning mechanism by pointlike defects, which is responsible for the significant improvement of the critical current behavior in the magnetic field.[35] We assumed that in the pristine sample the dominant pinning mechanism is by grain boundaries and that such contribution is unaffected by irradiation, so that it should rescale with the condensation energy of the sample $E_c = \mu_0 B_c^2(T) \approx \mu_0 B_c^2(0)(1-(T/T_c)^2)^2 \propto T_c^2(1-(T/T_c)^2)^2$. The rescaled grain boundary pinning contribution lies well below the experimental data for samples irradiated with fluence lower than 10^{18} cm^{-2}, that is, when the critical temperature is not depressed by more than 10%. The total current can be calculated as the sum of the rescaled grain boundary contribution plus a point defect contribution, with two free parameters: the point defects pinning multiplicative coefficient A_p and the anisotropy γ. The fitting results show that the anisotropy decreases with increasing fluence, with values around 4–4.5 for samples irradiated at fluences up to 10^{18} cm^{-2} (from P0 to P3.5), and around 1 for samples irradiated at larger fluences (from P4 to P6), while the coefficient A_p increases with fluence. In particular, A_p values scale with the $1/3$ power of the fluence; this is a check of the validity of this description, as A_p is indeed linearly related to the inverse of the average distance between point defect pinning centers induced by irradiation, which in turns is proportional to the $1/3$ power of the fluence. Instead, as confirmed also by new data on P3.5 and P3.7 samples, for fluences larger than 10^{18} cm^{-2} the rescaled grain boundary contribution is even larger than the experimental data points, indicating a failure of the scaling procedure. Work is in progress to understand the reason for such failure; we propose that it may be ascribed to two effects that we have neglected: the first one is the likely suppression in the density of states and the second one is the trend towards a single gap behavior in the most irradiated samples, as demonstrated in Ref. 36

By a close inspection of the shape of the curves in the main panel of Fig. 9, it can be noted that while for P0, P1, P2, the critical current density monotonically decreases with magnetic field, in the cases of P3, P3.5, P3.7 it presents a smooth plateau/upraise (well visible in linear scale). At larger fluences this feature progressively disappears. A similar, but more evident, upraise has been observed on irradiated single crystals[42] where the peak position is shifted to lower magnetic fields with increasing disorder; this fishtail effect has been attributed to an order-disorder transition of the flux line lattice. Also pinning by variations of the superconducting order parameter, either due to areas with depressed T_c or with depressed electron mean free path could result in a nonmonotonic behavior of the critical current density as a function of the magnetic field. Indeed, it may be that beside the already cited pointlike defects pinning mechanism, also a pinning mechanism by local variations of the superconducting order parameter could be induced by neutron irradiation. Such other mechanism should be considered to fit the whole shape of the curves; however the large number of free parameters makes unreliable any quantitative analysis, especially due to the fact that the original pinning contribution by grain boundaries of the unirradiated sample does not scale as expected with T_c for fluences larger than 10^{18} cm^{-2}. The single grain contribution to the critical current density $j_c^{(sg)}$ of the three different pinning mechanisms, namely by grain boundaries, by point defects and by variations of the superconducting order parameter, is shown in Fig. 10, as a function of the reduced field H/H_{c2}. It is evident that the presence of the latter mechanism could indeed account for the nonmonotonic magnetic field dependence of the sample critical current density, which results from the percolation process through randomly oriented grains.

VI. CHARACTERISTIC LENGTHS

Some characteristic lengths, namely the coherence length and the electron mean free path, can be estimated in the irradiated samples in order to shed light on the type of disorder introduced by irradiation.

We have noticed that, with the exception of the intermediate range of fluence, the transition widths of these samples

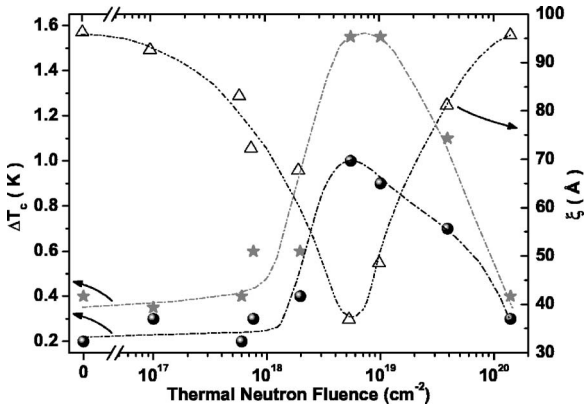

FIG. 11. Transition width ΔT_c ($T_{90\%}-T_{10\%}$, black circles, $T_{98\%}-T_{2\%}$, grey stars) and coherence length ξ (open symbols) as a function of thermal neutron fluence. The lines are guides for the eyes.

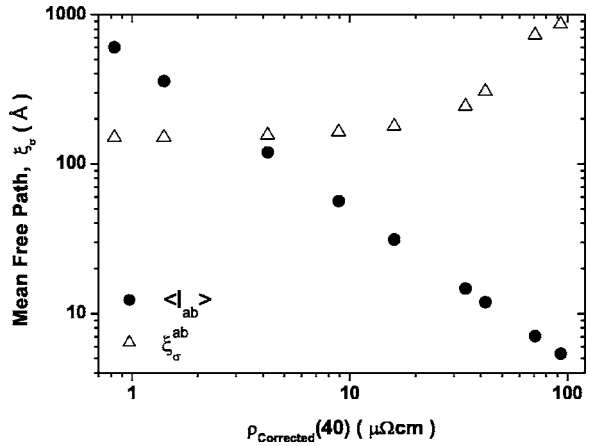

FIG. 12. In-plane BCS coherence length ξ_0 for the σ band (open symbols) and in-plane mean free path (solid symbols) as a function of corrected residual resistivity.

remain extraordinarily sharp despite the critical temperature is reduced by more than four times compared to the pristine value. This result is even more surprising as they have been observed also in the specific heat measurements[36] which are sensitive to all kinds of inhomogeneity. Moreover, it is interesting to note that P-3.7 and P-4 show a ΔT_c slightly larger than other samples and this is even true when ΔT_c is estimated by susceptibility and specific heat.[36]

The sharpness of transition is indicative that defects induced by irradiation are homogeneously distributed on the scale of the coherence length. The evaluation of the coherence length ξ cannot be obtained straightforwardly from H_{c2} because of the two band contributions. Anyway, we can estimate an effective value of ξ by the relation $\xi=\left[\frac{2\pi\Phi_0}{\mu_0 H_{c2}^{\|c}(0)}\right]^{1/2}$, where Φ_0 is quantum flux (2.07×10^{-15} T m^2) and $\mu_0 H_{c2}^{\|c}(0)$ is the upper critical field parallel to the c axis at zero temperature. As already said, in polycrystalline samples we measure the uppermost critical field, i.e., $\mu_0 H_{c2}^{\|ab}(0)$, and $\mu_0 H_{c2}^{\|c}(0)$ can be estimated as $\mu_0 H_{c2}^{\|ab}(0)/\gamma$ where γ comes from the J_c analysis.[35] The so derived ξ values are shown in Fig. 11 as a function of fluence. In spite of several approximations the result is clear, reflecting the behavior of the upper critical fields. Starting from the clean sample ($\xi\sim100$ Å), the coherence length decreases by increasing the disorder, as an effect of the suppression of the mean free path. A further increase of disorder suppresses T_c and therefore the condensation energy. This causes an enhancement of ξ, which reaches again a value of about 100 Å in the most irradiated sample.

The amplitude of the resistive transition, $\Delta T_c=T_{90\%}-T_{10\%}$, is plotted in the same graph (black circles); ΔT_c and ξ curves show a mirrorlike behavior. The transition width ΔT_c reaches its maximum, about 1 K, in the P-3.7 sample and, in the same sample, the coherence length has a minimum ($\sim$40 Å). In the most irradiated samples the transition is sharp again ($\Delta T_c\sim0.3$ K), being the coherence length raised to 100 Å. The strong correlation existing between ΔT_c and ξ indicates that when coherence length is much larger than the typical scale of defect inhomogeneity, the disorder is averaged out; on the contrary when the coherence length decreases (P-3.5, P-3.7, and P-4) the disorder is more effective in broadening the transition. Consistently with this scenario, the samples with smaller coherence lengths are the only ones whose critical current exhibits a broad bump characteristic of pinning by local inhomogeneity of the superconducting order parameter (see Sec. V). To verify that transition width behaviour is not influenced by the employed criterion, in Fig. 11 we also add data obtained by 4–98% of residual resistivity (grey stars); we note that the same trend is shown.

Another length that characterizes disordered samples is the electronic mean free path, l. In a two band system two different mean free paths, l_σ and l_π should be considered. If we are interested only to emphasize the behavior of l with disorder, an effective value can be extracted. We suppose, for simplicity, that the scattering rates in the two bands are the same ($\Gamma_\pi\sim\Gamma_o=\Gamma$); this assumption is quite reasonable in artificial disordered samples. The scattering rate can be evaluated by resistivity as $\Gamma=\varepsilon_0\rho(\omega_{P\sigma}^2+\omega_{P\pi}^2)$, where $\omega_{P\sigma}=6.23$ eV and $\omega_{P\pi}=3.40$ eV are the mean values of the plasma frequencies.[43] By the mean in-plane value of the Fermi velocity ($v_{F\sigma}\sim v_{F\pi}\sim5.1\times10^5$ m/s) we determine the mean free path $\langle l^{ab}\rangle$. $\langle l^{ab}\rangle$ (full symbols) is plotted as a function of corrected residual resistivity in Fig. 12. The initial value, 600 Å, indicates a very clean sample condition; then $\langle l^{ab}\rangle$ decreases down to few Å, the same order of magnitude of the cell size.

Finally, it could be interesting to compare the mean free path with the BCS coherence length (ξ_0) in order to verify the passage from the clean to the dirty limit in irradiated samples. The two band nature of MgB_2 does not allow an unambiguous definition of the dirty limit, even if it was proven that the increase of the upper critical field with respect to its intrinsic value occurs when σ bands become dirty ($l_\sigma<\xi_{0\sigma}$).[10] As discussed above, we are not able to estimate l_σ, while $\xi_{0\sigma}$ can be calculated from the energy gap of σ bands, $\Delta_\sigma(0)$ determined in Ref. 36 by employing the formula $\xi_{0\sigma}=\frac{\hbar v_{F\sigma}}{\pi\Delta_\sigma(0)}$. In Fig. 12 we report $\xi_{0\sigma}$ (open symbols): it ranges from 150 Å, in the pristine sample, to nearly 900 Å, in the most exposed one. In the limit of the rough approximations done, we can observe that in the pristine sample $\xi_{0\sigma}$

is close to the ξ estimated by the upper critical field. This confirms that unirradiated samples are in the clean limit[10] At fluence larger than 1.0×10^{17} cm^{-2}, H_{c2} increases and consequently ξ diminishes; this behavior implies the crossover from the clean to the dirty limit. In the dirty limit the coherence length ξ is related with the mean free path l and the BCS coherence length ξ_0 by the relation $\xi\approx(\xi_0 l)^{1/2}$. Thus, looking at Fig. 11, the nonmonotonic behavior of ξ can be nicely explained by the decrease of l at a low level of disorder, followed by the sharp increase of $\xi_{0\sigma}$ at a high level of disorder.

VII. CONCLUSION

We prepared three different series of high quality polycrystalline magnesium diboride by direct synthesis of pure elements. To avoid self-shielding, in the sample preparation we used boron with less than 0.5% ^{10}B, thus increasing penetration depth of neutrons up to 1 cm. The samples were irradiated with neutrons at two different facilities that have approximately the same thermal neutron flux density, but differing by three orders of magnitude in the fast neutron flux density. A series of samples was irradiated with the Cd shield to absorb thermal neutrons. The comparison of electrical and structural properties of the three sample series allowed us to conclude that the main damage mechanisms are caused by thermal neutrons, whereas fast neutrons play a minor role.

The critical temperature was reduced down to 9 K with a fluence of 1.4×10^{20} cm^{-2}; at the same time the normal state resistivity is increased by more than two orders of magnitude and the cell volume is considerably increased (1.7%). All the samples, even the most irradiated ones, showed a good level of homogeneity. This is proven by x-ray diffraction patterns, whose peaks remain very narrow up to the highest exposition level. Moreover, both in resistive and inductive measurements, the transition widths remain sharp, showing a broadening only in the intermediate range of fluence.

The upper critical field appears strongly influenced by irradiation. At low fluences H_{c2} increases exceeding 30 T at 2×10^{18} cm^{-2}, while the critical temperature is only slightly reduced. For higher fluences H_{c2} is suddenly reduced both as a consequence of a strong T_c suppression and the anisotropy reduction. We compared these data with the current literature ones and we observed a pronounced maximum in H_{c2} both in irradiated and C-doped samples at about 35 K of T_c.

We interpreted the H_{c2} data in the framework of an existing model for two bands superconductors; despite the fit quality is acceptable, the resistivity calculated from the obtained scattering times does not match perfectly with the measured one. The interband scattering might not be the only mechanism able to suppress superconductivity. Another likely mechanism is the weakening of electron-phonon coupling, as supported by specific heat measurements.

The critical current density as well undergoes the effect of neutron irradiation showing a nearly flat magnetic field dependence in a region as wide as several Teslas. The largest J_c improvement was obtained at the same exposition level, where the largest increase of the upper critical field was observed. We had clear evidence that, to take into account the evolution of J_c with fluence, it is necessary to include the contributions of more pinning mechanisms; pinning by grains boundaries, by pointlike defects and by local variations of the superconducting order parameter. The relative weight of these contributions changes as a function of fluence.

Finally, a correlation between coherence length and the transition width has been shown; we evaluated that in the samples with the larger coherence lengths the transition appears extremely sharp because disorder is averaged out, whereas in the samples with lower coherence lengths disorder is more effective in broadening the transition. Consistently with this scenario, samples with smaller coherence lengths are those whose critical current exhibits a broad bump characteristic of pinning by local inhomogeneity of the superconducting order parameter.

ACKNOWLEDGMENTS

We acknowledge the support of the European Commission from the 6th framework programme "Transnational Access-Specific Support Action," contract No. RITA-CT-2003-505474. This work is partially supported by the project No. PRIN2004

*Electronic address: tarantini@ge.infm.it

[1] J. Nagamatsu, N. Nakawaga, T. Muranaka, Y. Zenitani, and J. Akimitsu, Nature (London) **410**, 63 (2001).
[2] H. Suhl, B. T. Matthias, and L. R. Walker, Phys. Rev. Lett. **3**, 552 (1959).
[3] G. Binnig, A. Baratoff, H. E. Hoenig, and J. G. Bednorz, Phys. Rev. Lett. **45**, 1352 (1980).
[4] A. A. Golubov and I. I. Mazin, Phys. Rev. B **55**, 15146 (1997).
[5] A. Gurevich, Phys. Rev. B **67**, 184515 (2003).
[6] A. A. Golubov and A. E. Koshelev, Phys. Rev. B **68**, 104503 (2003).
[7] E. Ohmichi, E. Komatsu, T. Masui, S. Lee, S. Tajima, and T. Osada, Phys. Rev. B **70**, 174513 (2004).
[8] R. H. T. Wilke, S. L. Bud'ko, P. C. Canfield, D. K. Finnemore, R. J. Suplinskas, and S. T. Hannahs, Phys. Rev. Lett. **92**, 217003 (2004).
[9] V. Braccini, A. Gurevich, J. E. Giencke, M. C. Jewell, C. B. Eom, D. C. Larbalestier, A. V. Pogrebnyakov, Y. Cui, B. T. Liu, Y. F. Hu, J. M. Redwing, Qi Li, X. X. Xi, R. K. Singh, R. Gandikota, J. Kim, B. Wilkens, N. Newmann, J. Rowell, B. Moeckly, V. Ferrando, C. Tarantini, D. Marré, M. Putti, C. Ferdeghini, R. Vaglio, and E. Haanappel, Phys. Rev. B **71**, 012504 (2005).
[10] M. Putti, V. Braccini, C. Ferdeghini, I. Pallecchi, A. S. Siri, F. Gatti, P. Manfrinetti, and A. Palenzona, Phys. Rev. B **70**, 052509 (2004).
[11] J. Karpinski, N. D. Zhigadlo, G. Schuck, S. M. Kazakov, B. Bat-

logg, K. Rogacki, R. Puzniak, J. Jun, E. Müller, P. Wägli, R. Gonnelli, D. Daghero, G. A. Ummarino, and V. A. Stepanov, Phys. Rev. B **71**, 174506 (2005).

[12] M. Monni, C. Ferdeghini, P. Manfrinetti, A. Palenzona, M. Putti, M. Affronte, P. Postorino, M. Lavagnini, A. Sacchetti, D. Di Castro, F. Sacchetti, C. Petrillo, and A. Orecchini, cond-mat/0506162 (unpublished).

[13] R. Gandikota, R. K. Singh, J. Kim, B. Wilkens, N. Newman, J. M. Rowell, A. V. Pogrebnyakov, X. X. Xi, J. M. Redwing, S. Y. Xu, and Qi Li, Appl. Phys. Lett. **86**, 012508 (2005).

[14] R. Gandikota, R. K. Singh, J. Kim, B. Wilkens, N. Newman, J. M. Rowell, A. V. Pogrebnyakov, X. X. Xi, J. M. Redwing, S. Y. Xu, Q. Li, and B. H. Moeckly, Appl. Phys. Lett. **87**, 072507 (2005).

[15] S. R. Shinde, S. B. Ogale, J. Higgins, R. J. Choudhary, V. N. Kulkarni, T. Venkatesan, H. Zheng, R. Ramesh, A. V. Pogrebnyakov, S. Y. Xu, Qi Li, X. X. Xi, J. M. Redwing, and D. Kanjilal, Appl. Phys. Lett. **84**, 2352 (2004).

[16] Y. Bugoslavsky, L. F. Cohen, G. K. Perkins, M. Polichetti, T. J. Tate, R. Gwilliam, and A. D. Caplin, Nature (London) **411**, 561 (2001).

[17] G. K. Perkins, Y. Bugoslavsky, A. D. Caplin, J. Moore, T. J. Tate, R. Gwilliam, J. Jun, S. M. Kazakov, J. Karpinski, and L. F. Cohen, Supercond. Sci. Technol. **17**, 232 (2004).

[18] A. E. Kar'kin, V. I. Voronin, T. V. D'yachkova, N. I. Kadyrova, A. P. Tyutyunik, V. G. Zubkov, Yu. G. Zainulin, M. V. Sadovski, and B. N. Goshchitskii, JETP Lett. **73**, 570 (2001).

[19] R. H. T. Wilke, S. L. Bud'ko, P. C. Canfield, J. Farmer, and S. T. Hannahs, cond-mat/0507185 (unpublished).

[20] M. Eisterer, M. Zehetmayer, S. Tonies, H. W. Weber, M. Kambara, N. H. Babu, D. A. Cardwell, and L. R. Greenwood, Supercond. Sci. Technol. **15**, L9 (2002).

[21] M. Eisterer, Phys. Status Solidi C **5**, 1606 (2005).

[22] M. Putti, V. Braccini, C. Ferdeghini, F. Gatti, P. Manfrinetti, D. Marré, M. Monni, A. Palenzona, I. Pallecchi, C. Tarantini, I. Sheikin, H. U. Aebersold, and E. Lehmann, Appl. Phys. Lett. **86**, 112503 (2005).

[23] A. Palenzona, P. Manfrinetti, and V. Braccini, INFM Patent No. T02001A001098.

[24] S. L. Bud'ko, G. Lapertot, C. Petrovic, C. E. Cunningham, N. Anderson, and P. C. Canfield, Phys. Rev. Lett. **86**, 1877 (2001).

[25] D. K. Finnemore, J. E. Ostenson, S. L. Bud'ko, G. Lapertot, and P. C. Canfield, Phys. Rev. Lett. **86**, 2420 (2001).

[26] J. M. Rowell, Supercond. Sci. Technol. **16**, R17 (2003).

[27] Y. Wang, F. Bouquet, I. Sheikin, P. Toulemonde, B. Revaz, M. Eisterer, H. W. Weber, J. Hinderer, and A. Junod., J. Phys.: Condens. Matter **15**, 883 (2003).

[28] R. H. T. Wilke, S. L. Bud'ko, P. C. Canfield, D. K. Finnemore, Raymond J. Suplinskas, and S. T. Hannahs, Physica C **424**, 1 (2005).

[29] Z. Holanova, J. Kacmarcik, P. Szabo, P. Samuely, I. Sheikin, R. A. Ribeiro, S. L. Bud'ko, and P. C. Canfield, Physica C **404**, 195 (2004).

[30] C. Dynes and C. M. Varma, J. Phys. F: Met. Phys. **6**, L215 (1976).

[31] J. M. Rowell, in Proceedings of the European Conference of Applied Superconductivity (2005).

[32] V. Ferrando, P. Manfrinetti, D. Marré, M. Putti, I. Sheikin, C. Tarantini, and C. Ferdeghini, Phys. Rev. B **68**, 094517 (2003).

[33] V. Ferrando, C. Tarantini, P. Manfrinetti, D. Marré, M. Putti, A. Tumino, and C. Ferdeghini, in Proceedings of European Conference of Applied Superconductivity (2003).

[34] M. Iavarone, R. Di Capua, A. E. Koshelev, W. K. Kwok, F. Chiarella, R. Vaglio, W. N. Kang, E. M. Choi, H. J. Kim, S. I. Lee, A. V. Pogrebnyakov, J. M. Redwing, and X. X. Xi, Phys. Rev. B **71**, 214502 (2005).

[35] I. Pallecchi, C. Tarantini, H. U. Aebersold, V. Braccini, C. Fanciulli, C. Ferdeghini, F. Gatti, E. Lehmann, P. Manfrinetti, D. Marré, A. Palenzona, A. S. Siri, M. Vignolo, and M. Putti, Phys. Rev. B **71**, 212507 (2005).

[36] M. Putti, M. Affronte, C. Ferdeghini, P. Manfrinetti, C. Tarantini, and E. Lehmann, Phys. Rev. Lett. **96**, 077003 (2006).

[37] N. R. Werthamer, E. Helfand, and P. C. Hohenberg, Phys. Rev. **147**, 295 (1966).

[38] A. Gurevich, S. Patnaik, V. Braccini, K. H. Kim, C. Mielke, X. Song, L. D. Cooley, S. D. Bu, D. M. Kim, J. H. Choi, L. J. Belenky, J. Giencke, M. K. Lee, W. Tian, X. Q. Pan, A. Siri, E. E. Hellstrom, C. B. Eom, and D. C. Larbalestier, Supercond. Sci. Technol. **17**, 278 (2004).

[39] M. Putti, C. Ferdeghini, M. Monni, I. Pallecchi, C. Tarantini, P. Manfrinetti, A. Palenzona, D. Daghero, R. S. Gonnelli, and V. A. Stepanov, Phys. Rev. B **71**, 144505 (2005).

[40] I. Pallecchi, V. Ferrando, E. Galleani D'Agliano, D. Marré, M. Monni, M. Putti, C. Tarantini, F. Gatti, H. U. Aebersold, E. Lehmann, X. X. Xi, E. G. Haanappel, and C. Ferdeghini, Phys. Rev. B **72**, 184512 (2005).

[41] M. Eisterer, M. Zehetmayer, and H. W. Weber, Phys. Rev. Lett. **90**, 247002 (2003).

[42] M. Zehetmayer, M. Eisterer, J. Jun, S. M. Kazakov, J. Karpinski, B. Birajdar, O. Eibl, and H. W. Weber, Phys. Rev. B **69**, 054510 (2004).

[43] M. Putti, V. Braccini, E. Galleani, F. Napoli, I. Pallecchi, A. S. Siri, P. Manfrinetti, and A. Palenzona, Supercond. Sci. Technol. **16**, 188 (2003).